Application and Verification of a Dynamic Vector-Hysteresis Model

Simon Steentjes, Daniel Eggers, and Kay Hameyer

Institute of Electrical Machines (IEM), RWTH Aachen University, Aachen 52062 Germany

This paper presents the application and verification of a dynamic vector-hysteresis model for nonoriented ferromagnetic materials. The hysteresis model is based on the fundamental principles of thermodynamics. Since the model is completely consistent with a genuine energy interpretation it can be considered from this point of view as a mechanical analog. To validate the model, the response of the model is compared to measured material characteristics of an isotropic electrical steel grade.

***Index Terms*—Energy conservation, magnetic hysteresis, magnetic material modeling, vector-hysteresis model.**

I. Introduction

THE detailed understanding of soft magnetic materials is essential for the development of soft magnetic steels, the most appropriate material choice and for the optimization of electrical machine designs. For particular applications the most accurate prediction of iron losses is essential. Therefore, accurate modeling of the dynamic hysteresis loops is of importance for design engineers and material manufacturer. If the aim is the highest possible accuracy, the numerical integration of the iron losses in the field solution by a magneto-dynamic hysteresis model is required, i.e. a simultaneous solving of the magnetic field equations with consideration of magnetic hysteresis and eddy current effects. This enables the characterization of the magnetization behavior of magnetic materials under sinusoidal or distorted, unidirectional or rotating field conditions. Phenomenological hysteresis models such as the Preisach [1] or Jiles-Atherton model [2] are essentially interpolated measurements, which are adapted to the numerical field problem. The choice of their particular family of interpolation basis functions presides little physical consideration. Both models lack a true physical background and suffer in general from poor accuracy in the interesting ranges of flux density and frequency for electrical machine design, i.e., outside the measurement ranges used for the parameter identification. Many of the currently used hysteresis models are fundamentally scalar models and are solely vectorized to 2-D or 3-D quite artificially [3], [4]. An alternative approach treats the problem directly at the microscopic level and uses multi-scale techniques [5] to trace the microscopic information over to the macroscopic level. The microscopic scale is that of Weiss domains and Bloch walls. These techniques are definitely relevant to improve the understanding of the microscopic phenomena involved. However, considering their very high computational cost, they are impracticable in modeling engineering applications. The purpose of this paper is to introduce an energy-based modeling of magnetic materials [3], [4], [6] in order to characterize the nonlinear behavior of magnetic materials as well as the associated energy losses for any instant of time. This enables to go beyond the limitations of currently used models. For this purpose, the energy-based and intrinsical vector capable hysteresis model [3], [4] is further developed and implemented in Python [7] to work in the IEM in-house finite element software package iMOOSE.

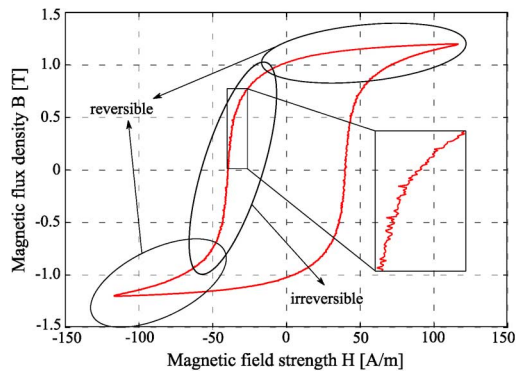

Fig. 1. Magnetic flux density $B(t)$ as a function of applied magnetic field $H(t)$. Enlarged are the Barkhausen jumps during the irreversible magnetization process.

II. Loss Mechanisms in Ferromagnetic Materials

The typical hysteresis behavior of soft magnetic materials is the macroscopic result of the magnetization process at the microscopic level. Each ferromagnetic material has a magnetic domain structure, which is closely associated with the magnetization process. Domains evolve since the system aims at a minimum free energy state following the principles of thermodynamics. Under the influence of an externally applied magnetic field the equilibrium of the free energy is disturbed and the domain structure rearranges itself. It is important to distinguish between three mechanisms resulting in magnetization changes:

1) reversible domain wall motion;
2) irreversible domain wall motion;
3) coherent rotation.

Irreversible domain wall motion is an abrupt movement from one energy minimum to another [1]. This leads to heat dissipation due to localized eddy currents. Those abrupt movements result in discontinuous changes of magnetization (Fig. 1) [1]. These jumps in magnetization are known as Barkhausen jumps. During reversible domain wall motion the micromagnetic system remains in a local energy minimum, but the position of this minimum varies with the applied magnetic field [1]. This leads to continuous changes in the magnetization. In saturation changes in magnetization are mainly reversible in nature, since the system is located in the global energy minimum.

Manuscript received March 02, 2012; revised May 04, 2012; accepted May 05, 2012. Date of current version October 19, 2012. Corresponding author: S. Steentjes (e-mail: simon.steentjes@iem.rwth-aachen.de).

Color versions of one or more of the figures in this paper are available online at http://ieeexplore.ieee.org.

Digital Object Identifier 10.1109/TMAG.2012.2199967

Metallic soft magnetic materials exhibit significant time-dependent effects under dynamic operating conditions. These lead to the complex nonlinear behavior of the magnetic hysteresis depending on the magnetization frequency and the peak value of the induction. Bulging of hysteresis loops arises through the movement of domain walls dampening microscopic eddy currents originating from abrupt change in energy [1]. Additionally the variation of the externally applied magnetic field induces macroscopic eddy currents.

III. Energy-Based Dynamic Vector-Hysteresis Model

The first law of thermodynamics (1) states that every system has an internal energy that can only be changed by the transport of work and/or heat beyond the boundaries of the system

$$\dot{\rho}^{\Psi} = \dot{\rho}^{W} + \dot{\rho}^{Q}. \tag{1}$$

A change in internal energy density $\dot{\rho}^{\Psi}$ corresponds to the work done on the system $\dot{\rho}^{W}$ plus the emitted or absorbed heat $\dot{\rho}^{Q}$. The used dynamic vector-hysteresis model [3], [4] builds on the thermodynamic representation of hysteresis. Thermal effects are neglected since entropy is assumed to be constant.

The internal energy corresponds to a reversible magnetic field strength $\vec{h}_r$ and the dissipated work within the system to an irreversible magnetic field strength $\vec{h}_{irr}$. Therewith the energy densities are described by

$$\dot{\rho}^{\Psi} = \vec{h}_r \cdot \dot{\vec{M}} \tag{2}$$

$$\dot{\rho}^{Q} = \vec{h}_{irr} \cdot \dot{\vec{M}}. \tag{3}$$

Deriving the energy dissipation functional (3) with respect to $\dot{\vec{M}}$ makes it possible to represent the energy balance as a function of the magnetic field strength

$$\vec{h} = \vec{h}_r + \vec{h}_{irr}. \tag{4}$$

In order to separately treat pure hysteresis losses and dynamic losses, the irreversible magnetic field strength is separated into two parts $\vec{h}_i$ and $\vec{h}_j$. At the macroscopic level the microscopic distribution of the pinning points, hindering the domain wall motion, cannot be modeled explicitly. Letting the number of ripples in the energy density functions tend to infinity, the pinning force can be modeled as an analog by a dry friction force κ as in the Jiles-Atherton model [2], [6]. This force counteracts any change in magnetization and the corresponding energy density is converted into heat. Hence the pure hysteresis losses are represented by a dry friction force of constant amplitude [3], [4]

$$\vec{h}_i = \frac{\partial}{\partial \dot{\vec{M}}} \left(\kappa \cdot |\dot{\vec{M}}| \right) \in G. \tag{5}$$

Since the energy dissipation functional is not differentiable, it models the memory effect. But (5) is a convex function and thus there exists a subgradient G [3], [4].

Considering the dynamics of the magnetization process, the attenuation by microscopic eddy currents can be represented as an mechanical analog by a movement with viscous friction with the friction constant λ

$$\vec{h}_j = \frac{1}{2} \frac{\partial}{\partial \dot{\vec{M}}} (\lambda \cdot \dot{\vec{M}}^2). \tag{6}$$

This makes it possible to specify the macroscopic magnetization with consideration of hysteresis

$$\vec{B}(\vec{h}) = \vec{M}(\vec{h}_r) + \mu_0 \cdot \vec{h}. \tag{7}$$

The magnetization $\vec{M}(\vec{h}_r)$ is described by a parametric saturation curve, whose parameters are identified from measurements. A well-known, physical based description for nonoriented steels is the Langevin function [3], [4]. Two Langevin functions are chosen to describe the anhysteretic magnetization curve (8). The anhysteretic curve describes the thermodynamic equilibrium and therewith the reversible magnetization. The first one represents the region of the anhysteretic curve, where the motion of Bloch walls is dominating, the second one the rotation of the magnetic moments relative to the preferred axis (coherent rotation)

$$M(h_r) = M_{s,bw} \cdot \left(\coth\left(\frac{3\mu_{bw} h_r}{M_{s,bw}} \right) - \frac{M_{s,bw}}{3\mu_{bw} h_r} \right) + M_{s,cr} \cdot \left(\coth\left(\frac{3\mu_{cr} h_r}{M_{s,cr}} \right) - \frac{M_{s,cr}}{3\mu_{cr} h_r} \right). \tag{8}$$

Equation (8) gives two degrees of freedom for the ferromagnetic characteristics (μ_{bw}, μ_{cr}) and two degrees of freedom for the saturation curve $(M_{s,bw}, M_{s,cr})$. Other functions to describe the anhysteretic curve are presented in [4]. It is important to point out that $h_r \neq h$. Finally the hysteresis model can be modeled as an analog in terms of a mechanical system [3], [4].

Under real conditions in polycrystalline materials, the domain structure is complex and statistical distributed pinning points are present. Correlation fields between adjacent domain walls determine the magnetization process and lead to large magnetization groups represented by the correlated motion of a large number of domain wall segments in a finite region in the material [1]. In order to represent the statistical distribution of the pinning point strength (local coercive forces) it is reasonable to assume that the magnetization is a multi-scale function, depending on the global value $|\vec{h}_r|$, which is composed of local values $\vec{h}_r^{\kappa}$ as follows:

$$|\vec{h}_r| = \left| \sum_k w^{\kappa} \cdot \vec{h}_r^{\kappa} \right| \tag{9}$$

with the weighting w

$$1 = \sum_k w^k. \tag{10}$$

This can be accounted for in the model by combining several elementary parts, called cells, and defining for each part a time-independent pinning force κ^k.

Therewith the global scale can be treated independently from the local scale. This independence enables a simple algorithm at the local scale. Each cell can be initiated independently and assigned to a local coercive force (i.e. local friction force κ^k). The viscous friction force acts on all cells similarly. This is modeled by a material dependent global friction constant λ. These $\vec{h}_r^{\kappa}$'s are the internal variables and they are all subjected to the same applied magnetic field $\vec{h}$. The equilibrium (4) can be written as a sum of independent cell-based magnetic fields

$$\vec{h} = \sum_k w^k \cdot \left(\vec{h}_r^k + \vec{h}_j^k \right) + \sum_k w^k \cdot \vec{h}_i^k \quad \forall\, \vec{h}_i^k \in G^k. \tag{11}$$

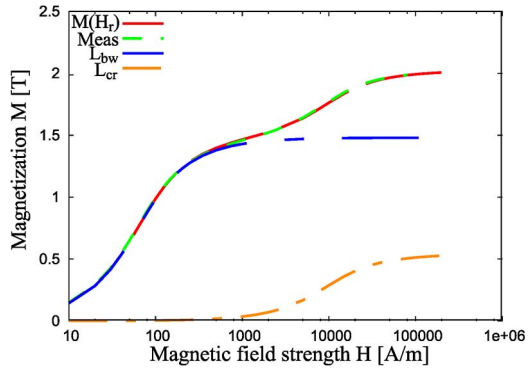

Fig. 2. Comparison of measured and extrapolated anhysteretic magnetization curve (measured) for M270-35A electric steel measured at the single sheet tester with the fitted double Langevin function $M(H_r)$.

TABLE I
LANGEVIN PARAMETERS FOR M270-35A

$M_{s,bw}$	$M_{s,cr}$	μ_{bw}	μ_{cr}
1.4404 T	0.5413 T	$53.401 \cdot 10^{-3}$	$0.1065 \cdot 10^{-3}$

IV. IDENTIFICATION OF THE FREE PARAMETERS

The free parameters of the vector-hysteresis model are identified using measured material characteristics on a standard Epstein frame (or single sheet tester).

A. Automatic Curve Fitting of the Anhysteretic Curve

Central material characteristic is the anhysteretic curve. Fig. 2 shows a comparison of the fitted double Langevin function with the measured and extrapolated anhysteretic curve for a nonoriented ferromagnetic steel sample (M270-35A). The double Langevin characteristic and the shift between the anhysteretic and initial magnetization curve due to irreversible effects in the range of small to medium magnetic polarizations is recognized. To identify the parameters of (8) the analytic double Langevin function is least-square fitted to the extrapolated measured anhysteretic magnetization curve (Table I). Separately shown in Fig. 2 are the first summand of the sum in (8) L_{bw} and the second summand L_{cr}.

B. Interpolation of the Coercive Curve $H_c(H)$

The identification of the local pinning forces κ^k and their weightings w^k is done by interpolating the coercive curve by a staircase function [4], which describes the abrupt, discontinuous magnetization process. The coercivity explicitly represents the lag of the reversible magnetic field $\vec{h}_r$ behind the externally applied field $\vec{h}$. Two interpolation methods are used: 1. *Spline interpolation* 2. *Optimal interpolation* with a modified Heaviside function.

The value $H(H_{c,k})$, the trigger point of the associated fraction, corresponds to the value of the respective friction coefficient κ^k [4]. The weighting of the cells, generally representing the probability of occurrence of the associated pinning force is obtained by the normalized rate of change dh/dh_c

$$w^k = \frac{1}{\sum_{k=1}^{n} \frac{dh^k}{dh_c^k}} \cdot \frac{dh^k}{dh_c^k} \tag{12}$$

TABLE II
MODEL PARAMETERS FOR M270-35A

κ^1	w^1	κ^2	w^2	κ^3	w^3	κ^4	w^4	κ^5	w^5
0.0	0.05	5	0.14	25.3	0.755	289	0.05	2000	0.005

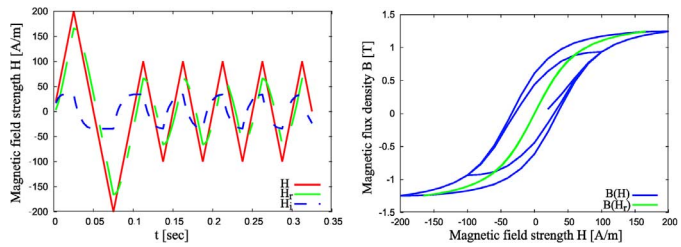

Fig. 3. Variation of the magnetic field (left) and resulting hysteresis loop (right).

To describe the domain wall bowing a cell with $\kappa^1 = 0$ is used. The global energy minimum is taken into account by a cell with $\kappa^n = H(H_{c,\max})$. In the future, a microstructural analysis of the distribution function of the pinning points will serve for the determination and identification of the weighting of individual cells. The identified parameters for M270-35A are listed in Table II.

C. Identification of the Viscous Friction Constant λ

The global viscous friction constant describing dynamic magnetization effects is currently identified by a try&error fitting with measured hysteresis loops and losses.

V. ANALYSIS AND VERIFICATION OF THE HYSTERESIS MODEL

A. Internal and Minor Loops, Stability Analysis

The model is able to reproduce stable internal loops. If the externally applied magnetic field is successively increased the ferromagnetic material is continuously magnetized. During this magnetization process internal loops are traversed. These internal loops are correctly modeled by the dynamic vector-hysteresis model. Furthermore stable minor loops can be modeled.

To study the stability of the hysteresis model the applied magnetic field oscillates at first between the main hysteresis loop and then around an internal loop (Fig. 3). The vector-hysteresis model provides a stable loop within the main loop and the turning point rule is adhered. Additionally a stable minor loop is obtained if the applied magnetic field alternates between two positive values as long as the turning point values stay unchanged.

B. Vector Fields

The magnetic field strength vector $\vec{H}(t)$ is described in the 2-D case by

$$H_x(t) = H_x \cdot \sin(\omega t) \tag{13}$$
$$H_y(t) = H_y \cdot \cos(\omega t) \tag{14}$$

with the angular velocity ω. Although the parameters of the vector-hysteresis model are identified using standard uniaxial measurements the model is able to reproduce the material behavior of isotropic materials under generally rotating or elliptical fields (Fig. 4).

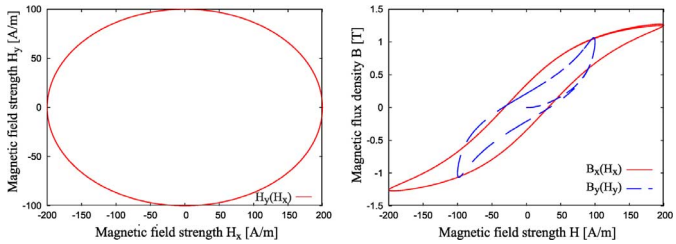

Fig. 4. Variation of the magnetic field (left) and resulting hysteresis loop (right).

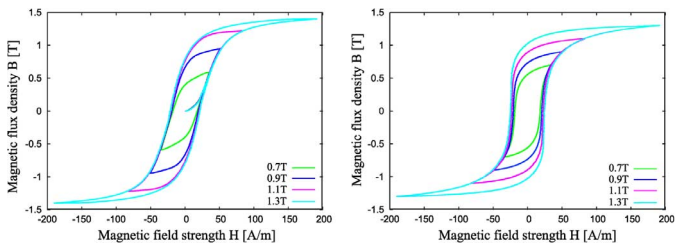

Fig. 5. Comparison of modeled (left) and measured (right) hysteresis loops for M270-35A at 3 Hz.

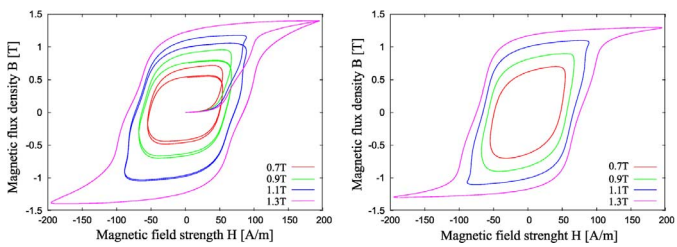

Fig. 6. Comparison of modeled (left) and measured (right) hysteresis loops for M270-35A at 200 Hz.

C. Verification Using Quasi-Static and Higher Frequency Measurements

To validate the identified parameters, the response of the hysteresis model is compared with measured material characteristics. A comparison of the measured losses as well as the magnetic hysteresis loops is conducted. An independent analysis of the parameters κ and w from the dynamic parameter λ is presented. Therefore quasi-static measurements and higher frequency measurements are analyzed. The magnetic field $H_{\mathrm{meas}}(t)$ used on the Epstein frame or single sheet tester serves as the model input. The model response $B_{\mathrm{mod}}(H_{\mathrm{meas}})$ obtained from (7) is compared to the measurement $B_{\mathrm{meas}}(H_{\mathrm{meas}})$ (Fig. 5). Deviations mainly occur in the medium polarization region and a significant shearing of the modeled hysteresis loop is apparent. Both effects are closely related to the modeling of the first Langevin function (8) as the central material characteristics of the model. The model reacts sensitive to the description of the reversible magnetization. The hysteresis model describes the bulging of the hysteresis loops using a single global constant parameter λ. The agreement is qualitatively higher than for the quasi-static measurements. Comparing higher-frequency hysteresis loops with each other, a good agreement between measured and modeled curves is obtained (Figs. 6 and 7).

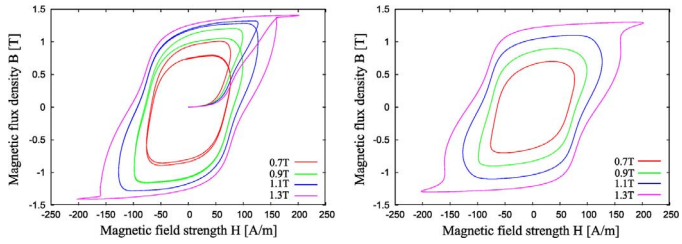

Fig. 7. Comparison of modeled (left) and measured (right) hysteresis loops for M270-35A at 400 Hz.

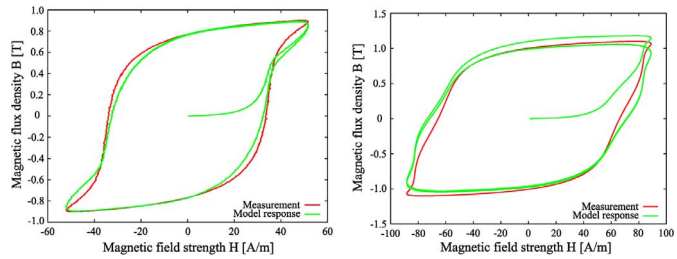

Fig. 8. Direct comparison of modeled and measured hysteresis loops for M270-35A at 50 Hz and 0.9 T (left) and 200 Hz and 1.1 T (right).

Direct comparisons of modeled and measured hysteresis loops are exemplarily shown for 50 Hz and 200 Hz for mid-level flux densities in Fig. 8.

VI. Conclusion

The vector-hysteresis model describes the metrological characteristics of nonoriented electrical steel accurately. A separate analysis of the different model parameters is presented. Further work is required regarding the physical justification of the parameter identification and the modeling of the anhysteretic curve to enable a more accurate modeling of hysteresis curves at various frequencies and magnetic flux density levels. This work is in progress. Anisotropy, i.e. oriented steel grades, can be considered by adding a weighting function of the angle of each individual magnetic moment with respect to the field. The proposed model in combination with a 1-D eddy current model of the half sheet thickness is a strongly coupled transient problem that enables nearly the exact calculation of the magnetic fields and losses. This will be realized in the next steps of this research work.

References

[1] G. Bertotti, *Hysteresis in Magnetism: For Physicists, Materials Scientists and Engineers*, I. Mayergoyz, Ed. New York: Academic, 1998.
[2] D. C. Jiles and D. L. Atherton, "Theory of ferromagnetic hysteresis," *J. Magn. Magn. Mater.*, vol. 61, pp. 48–60, 1986.
[3] F. Henrotte and K. Hameyer, "A dynamical vector hysteresis model based on an energy approach," *IEEE Trans. Magn.*, vol. 42, no. 4, pp. 899–902, Apr. 2006.
[4] F. Henrotte, A. Nicolet, and K. Hameyer, "An energy-based vector hysteresis model for ferromagnetic materials," *COMPEL*, vol. 25, no. 1, pp. 71–80, 2006.
[5] B. van de Wiele *et al.*, "Energy considerations in a micromagnetic hysteresis model and the preisach model," *J. Appl. Phys.*, vol. 108, 2010.
[6] A. Bergqvist, "Magnetic vector hysteresis model with friction-like pinning," *Phys. B*, vol. 233, pp. 342–347, 1997.
[7] [Online]. Available: http://www.python.org